ISTS-2017-d-106／ISSFD-2017-106

Optimal Trajectory Design of Formation Flying based on Attractive Sets

By Motoki YAMANE,[1)] Mai BANDO,[1)] and Shinji HOKAMOTO[1)]

[1)]*Department of Aeronautics and Astronautics, Kyushu University, Fukuoka, Japan*

This paper presents a new method of optimal trajectory design for formation flying. Under linearized assumptions and a quadratic performance index, we consider an attractive set for optimal control based on the linear quadratic regulator theory. An attractive set is defined as a set of all initial states to reach a desired state for a given cost. In particular, we define attractive sets for two problems: a fixed final-state, fixed final-time problem and an infinite-time problem. The properties of the two problems are investigated by plotting the attractive sets for each problem. Our results reveal that the L_1-norm of the finite-time problem is close to that of the infinite-time problem even though the flight time is much smaller.

Key Words: Spacecraft, Formation Flying, Optimal Control

Nomenclature

A	:	state matrix
B	:	input matrix
C	:	a constant
J	:	performance index
J^*	:	minimum value of performance index
n	:	mean motion
Q, R	:	weight matrices
$\boldsymbol{R}_c$	:	radius vector of chaser orbit
$\boldsymbol{R}_0$	:	radius vector of target orbit
T	:	orbital period
$\boldsymbol{u}$	:	control input vector
$\boldsymbol{u}^*$	:	optimal control input vector
$\boldsymbol{x}$	:	state vector
x, y, z	:	position
$\boldsymbol{\varepsilon}$	:	acceptable error range
μ	:	geocentric gravity constant
Subscripts		
0	:	initial
f	:	final
conv	:	convergence

1. Introduction

The Hill's equations (also known as the Hill-Clohessy-Wiltshire (HCW) equations) are equations of relative motion of a chaser linearized around a target.[1)]The Hill's equations have periodic solutions that are convenient for formation flying. The rendezvous problem for a target on a circular orbit has been investigated in various ways.[2)] The optimal rendezvous problem using continuous thrust is often treated as the optimal control problem. In constructing a feedback control system for a rendezvous problem, a linear quadratic regulator is often used.[3,4)] A linear quadratic regulator is a control law that minimizes a quadratic performance index for a linear system. Once the initial and final states are specified, the optimal trajectory can be obtained based on linear quadratic regulator theory. However, when using this method, it is necessary to solve the two-point boundary-value problem (TPBVP) repeatedly to determine the optimal initial state. To solve the TPBVP for rendezvous problem, the generating functions which give the optimal control as a function of initial and final state are used to find the optimal initial state in Refs. 5) and 6).

We present a new method of optimal trajectory design for formation flying. Under linearized assumptions and a quadratic performance index, we consider an attractive set for optimal control based on linear quadratic regulator theory. An attractive set is defined as a set of all initial states to reach a desired state for a given cost. Using the attractive set for optimal trajectory design, we not only can obtain the optimal initial conditions uniquely but also the structure behind it.

In a real mission, it is desirable to complete an orbit transfer in finite time. Therefore, this paper reveals the relation between the shape of an attractive set and an optimal trajectory for different boundary conditions. First, we define attractive sets for two optimal control problems: a fixed final-state, fixed final-time problem and an infinite-time problem. Next, by plotting an attractive set on a chaser's initial orbit, we compare the shape of the attractive set with the trajectory when termination time is changed. Moreover, we evaluate the obtained trajectory using the L_1-norm of the control input and compare the L_1-norm with the rendezvous completion time t_{conv}.

2. Equations of Motion

We consider relative motion between a target and a chaser on a circular orbit. Figure 1 shows the chaser's equations of motion relative to a target assuming the coordinate system (x, y, z) as follows:

$$\ddot{x} = 2n\dot{y} + n^2(R_0 + x) - \frac{\mu}{R^3}(R_0 + x) + u_x \tag{1}$$

$$\ddot{y} = -2n\dot{x} + n^2 y - \frac{\mu}{R^3}y + u_y \tag{2}$$

$$\ddot{z} = -\frac{\mu}{R^3}z + u_z \tag{3}$$

When these equations are linearized at the origin, Eqs. (1) to (3) become

$$\ddot{x} = 3n^2 x + 2n\dot{y} + u_x \tag{4}$$

$$\ddot{y} = -2n\dot{x} + u_y \tag{5}$$

$$\ddot{z} = -n^2 z + u_z \tag{6}$$

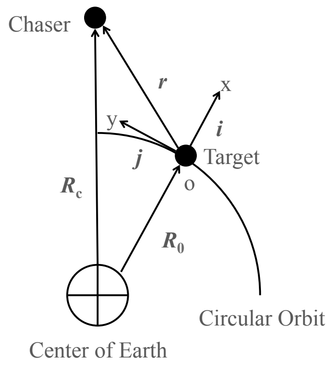

Fig. 1. Definition of coordinate system.

These equations are called Hill's equations.[1)]

Let $\boldsymbol{x} = [x, y, z, \dot{x}, \dot{y}, \dot{z}]^{\mathrm{T}}$ and $\boldsymbol{u} = [u_x, u_y, u_z]^{\mathrm{T}}$ be a state vector and an input vector, respectively. The Hill's equations can then be represented by

$$\dot{\boldsymbol{x}} = A\boldsymbol{x} + B\boldsymbol{u}, \quad \boldsymbol{x}(0) = \boldsymbol{x}_0 \tag{7}$$

where

$$A = \begin{pmatrix} 0 & 0 & 0 & 1 & 0 & 0 \\ 0 & 0 & 0 & 0 & 1 & 0 \\ 0 & 0 & 0 & 0 & 0 & 1 \\ 3n^2 & 0 & 0 & 0 & 2n & 0 \\ 0 & 0 & 0 & -2n & 0 & 0 \\ 0 & 0 & -n^2 & 0 & 0 & 0 \end{pmatrix} \tag{8}$$

$$B = \begin{pmatrix} 0 & 0 & 0 \\ 0 & 0 & 0 \\ 0 & 0 & 0 \\ 1 & 0 & 0 \\ 0 & 1 & 0 \\ 0 & 0 & 1 \end{pmatrix} \tag{9}$$

For simplicity, we only consider in-plane motion. Solving Eqs. (4) and (5) under $\boldsymbol{x}_0 = [x_0, y_0, \dot{x}_0, \dot{y}_0]^{\mathrm{T}}$, $\boldsymbol{u} = 0$ yields

$$x = (-3x_0 - \frac{2}{n}\dot{y}_0)c + \frac{\dot{x}_0}{n}s + 4x_0 + \frac{2}{n}\dot{y}_0 \tag{10}$$

$$y = \frac{2}{n}\dot{x}_0 c + (6x_0 + \frac{4}{n}\dot{y}_0)s + (-6nx_0 - 3\dot{y}_0)t + y_0 - \frac{2}{n}\dot{x}_0 \tag{11}$$

$$\dot{x} = \dot{x}_0 c + (3nx_0 + 2\dot{y}_0)s \tag{12}$$

$$\dot{y} = 2(3nx_0 + 2\dot{y}_0)c - 2\dot{x}_0 s - 3(2nx_0 + \dot{y}_0) \tag{13}$$

where $c \equiv \cos nt$, $s \equiv \sin nt$. From Eqs. (10) to (13), in the case where the secular term is equal to zero, a periodic solution is obtained:

$$\dot{y}_0 = -2nx_0 \tag{14}$$

Under this condition, Eqs. (10) to (13) express an elliptic orbit. The velocity $(\dot{x}, \dot{y})$ on the elliptic orbit at any position (x, y) is

$$\dot{x} = \frac{n}{2}y \tag{15}$$

$$\dot{y} = -2nx \tag{16}$$

3. Problem Statement and Definition of an Attractive Set

3.1. Fixed final-state, fixed final-time problem

Consider an optimal control problem for Eq. (7) that minimizes the performance index J given by

$$J = \int_{t_0}^{t_f} (\boldsymbol{x}^{\mathrm{T}} Q \boldsymbol{x} + \boldsymbol{u}^{\mathrm{T}} R \boldsymbol{u}) dt \tag{17}$$

where $Q \geq 0, R > 0$ and $\boldsymbol{x}(t_f) = \boldsymbol{x}_f$. The optimal control input that minimizes the performance index is as follows:[7)8)]

$$\boldsymbol{u}^* = -R^{-1}B^{\mathrm{T}}\{S(t)\boldsymbol{x} - U(t)W^{-1}(t_0)(U^{\mathrm{T}}(t_0)\boldsymbol{x}_0 - \boldsymbol{x}_f)\} \tag{18}$$

where S, U, and W are positive-definite solutions that satisfy the following equations:

$$\dot{S} + A^{\mathrm{T}}S + SA - SBR^{-1}B^{\mathrm{T}}S + Q = 0 \tag{19}$$

$$\dot{U} = -(A^{\mathrm{T}} - SBR^{-1}B^{\mathrm{T}})U \tag{20}$$

$$\dot{W} = U^{\mathrm{T}}BR^{-1}B^{\mathrm{T}}U \tag{21}$$

$$S(t_f) = \boldsymbol{O}, \quad U(t_f) = \boldsymbol{I}, \quad W(t_f) = \boldsymbol{O} \tag{22}$$

Then the minimum value of the performance index J^* is as follows:[7)9)]

$$J^* = \boldsymbol{x}_0^{\mathrm{T}} S(t_0) \boldsymbol{x}_0 - (\boldsymbol{x}_0^{\mathrm{T}} U_0 - \boldsymbol{x}_f^{\mathrm{T}}) W^{-1}(t_0)(U_0^{\mathrm{T}}\boldsymbol{x}_0 - \boldsymbol{x}_f) \tag{23}$$

Equation (23) expresses an n-dimensional ellipsoid. Consider the set of all initial state inside the n-dimensional ellipsoid $J^* = C$

$$\mathscr{A}(C) = \{\boldsymbol{x}_0 \in \boldsymbol{R}^n \mid \boldsymbol{x}_0 S(t_0)\boldsymbol{x}_0 - (\boldsymbol{x}_0^{\mathrm{T}} U_0 - \boldsymbol{x}_f^{\mathrm{T}}) W^{-1}(t_0)(U_0^{\mathrm{T}}\boldsymbol{x}_0 - \boldsymbol{x}_f) \leq C\} \tag{24}$$

We define $\mathscr{A}(C)$ as the attractive set for optimal control.[10)] The optimal trajectory departing from the inside of this ellipsoid is guaranteed that the value of the performance index is less than C.

3.2. Free final-state, fixed final-time problem

Consider an optimal control problem for Eq. (7) that minimizes the performance index J given by

$$J = \boldsymbol{x}_0^{\mathrm{T}} Q_0 \boldsymbol{x}_0 + \int_{t_0}^{t_f} (\boldsymbol{x}^{\mathrm{T}} Q \boldsymbol{x} + \boldsymbol{u}^{\mathrm{T}} R \boldsymbol{u}) dt \tag{25}$$

where $Q_0, Q \geq 0, R > 0$. The optimal control input that minimizes the performance index is as follows:

$$\boldsymbol{u}^* = -R^{-1}B^{\mathrm{T}}S(t)\boldsymbol{x} \tag{26}$$

where S is a positive definite solution satisfying the Riccati equation:

$$\dot{S} + A^{\mathrm{T}}S + SA - SBR^{-1}B^{\mathrm{T}}S + Q = 0 \tag{27}$$

$$S(t_f) = Q_0 \tag{28}$$

Then the minimum value of the performance index J^* is as follows:

$$J^* = \boldsymbol{x}_0^{\mathrm{T}} S(t_0) \boldsymbol{x}_0 \tag{29}$$

3.3. Infinite-time problem

Consider an optimal control problem for Eq. (7) that minimizes the performance index J given by

$$J = \int_{t_0}^{\infty} (\boldsymbol{x}^{\mathrm{T}} Q \boldsymbol{x} + \boldsymbol{u}^{\mathrm{T}} R \boldsymbol{u}) dt \tag{30}$$

where $Q \geq 0, R > 0$. The optimal control input that minimizes the performance index is as follows:

$$\boldsymbol{u}^* = -R^{-1} B^{\mathrm{T}} S \boldsymbol{x} \tag{31}$$

where S is a positive definite solution satisfying the algebraic Riccati equation:

$$A^{\mathrm{T}} S + SA - SBR^{-1} B^{\mathrm{T}} S + Q = 0 \tag{32}$$

Then the minimum value of the performance index J^* is as follows:

$$J^* = \boldsymbol{x}_0^{\mathrm{T}} S(t_0) \boldsymbol{x}_0 \tag{33}$$

The attractive set for optimal control is defined as

$$\mathscr{A}(C) = \{\boldsymbol{x}_0 \in \boldsymbol{R}^n \mid \boldsymbol{x}_0 S(t_0) \boldsymbol{x}_0 \leq C\} \tag{34}$$

4. Simulation Results

We use the equations of motion where Eq. (7) is dimensionless with $\boldsymbol{R}_0$ and $T \left(= \sqrt{\frac{\mu}{\boldsymbol{R}_0^3}}\right)$. Namely,

$$A = \begin{pmatrix} 0 & 0 & 1 & 0 \\ 0 & 0 & 0 & 1 \\ 3 & 0 & 0 & 2 \\ 0 & 0 & -2 & 0 \end{pmatrix} \tag{35}$$

$$B = \begin{pmatrix} 0 & 0 \\ 0 & 0 \\ 1 & 0 \\ 0 & 1 \end{pmatrix} \tag{36}$$

We consider a feedback control system in which the chaser rendezvouses to a target using thruster input and two optimal control problems that have different boundary conditions, respectively: a fixed final-state, fixed final-time problem and an infinite-time problem. The relation between the solution to the free final-state problem given by Eq. (26) is investigated in 4.3.1. For these two optimal control problems, we draw attractive sets for the initial values on the initial periodic orbit and compare these attractive sets. The chaser has the initial values $\boldsymbol{x}_0 = [1.0, 0, 0, -2.0]^{\mathrm{T}}$ on the initial periodic orbit. Let the initial maneuver time be t_0 and the termination time be t_f. In fact, in the infinite-time problem, it takes an infinite amount of time to complete the rendezvous. However, we set the acceptable error range $\boldsymbol{\varepsilon}$ and consider the time when it becomes less than $\boldsymbol{\varepsilon}$ as the rendezvous completion time t_{conv}.

$$\boldsymbol{\varepsilon} = [1.0, 1.0, 1.0, 1.0]^{\mathrm{T}} \times 10^{-3} \tag{37}$$

4.1. Basic properties of attractive sets for finite-time problem

For the finite-time problem, we set $\boldsymbol{x}_f = [0, 0, 0, 0]^{\mathrm{T}}$, $t_f = 3, 6, 9$. Let $Q = 10^q \boldsymbol{I}_{4\times4}$, $R = \boldsymbol{I}_{2\times2}$, and change the weight parameter of the state by decreasing the value of q. Figures 2 - 4 show the contour of the attractive set (24) (multicolored ellipses) and the optimal trajectory (red line).

First, consider the general properties of the optimal trajectory obtained by using a linear quadratic regulator. Paying attention to the red line in Figs.2 - 4, it is found that changing the weight parameter of the state changes the trajectory from straight to spiral and lengthens the route.

For the in-plane motion the attractive set is a four-dimensional ellipsoid of position and velocity; however, on a periodic orbit, the velocity of the chaser is a function of position through to Eqs. (15) and (16). Hence, the intersection of the ellipsoid and a periodic orbit is a two-dimensional ellipsoid, and can be drawn as an ellipse on the x-y plane. By plotting this ellipsoid on x-y plane, the value of the performance index along a periodic orbit can be determined uniquely. Figures 2 to 4 show that an attractive set has a distribution such that the value of the performance index increases from the inside to the outside of the ellipse. Moreover, Fig. 5 shows the values of J^* corresponding to the initial position on the periodic orbit for Fig. 2(c). In Fig. 5, J^* takes its minimum values at $y = \pm 2$. From Figs. 2(c) and 5, it is also found that the minimum values of the performance index are on points of contact between the periodic orbit and this ellipse.

The advantage of plotting an attractive set is that it is not necessary to repeat the calculation for the optimal trajectory by changing the initial state. Once we obtain the solution of the Riccati equation by solving Eqs. (19) to (21) (Eq. (32) in the case of the infinite-time problem) we obtain the optimal initial state immediately.

4.2. Basic properties of attractive sets for infinite-time problem

Figure 6 shows the contour of the attractive set (34) of the infinite-time problem for the different weight parameters. The properties of the attractive set described in 4.1 hold for the infinite-time problem. Moreover, the attractive set for the infinite-time problem with small q has a remarkable feature. In Fig. 6, it is observed that the contour of the attractive set converges to 2:1 ellipse for $Q \to 0$ and overlap with periodic orbits of Hill's equation. This means that the value of J^* remains almost unchanged wherever the chaser depart from the periodic orbit. Moreover, Fig. 7 shows the values of J^* by changing the initial position on the periodic orbit corresponding to Fig. 6(c). It is also found that the value of J^* is almost constant on the periodic orbit from Fig. 7. The larger the weight of the control input, the closer the trajectory is to the solution of the Hill's equations, which do not use control input.

This interesting property of attractive set can also be observed for different situation. Consider the attractive set for infinite-time problem when the initial velocity of the chaser is zero, i.e. $x_0 = [x, y, 0, 0]$. Note that the solutions starting from $x_0 = [x, y, 0, 0]$ has drift motion along y-axis from Eq. (11). Figure 8 shows the contour of the attractive set for different weight parameters. The attractive set becomes unbounded in y-

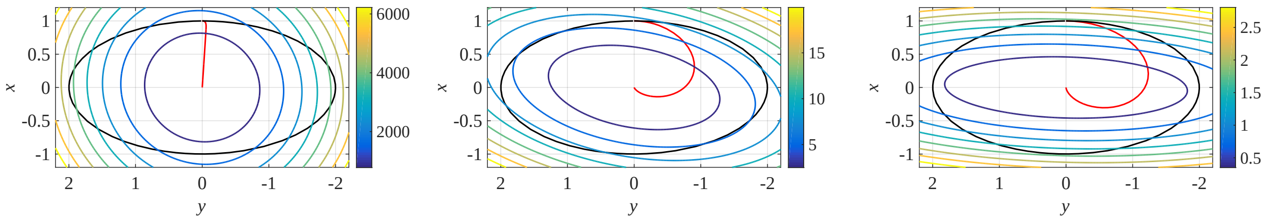

(a) $q = 3$. (b) $q = 0$. (c) $q = -3$.

Fig. 2. $t_f = 3$.

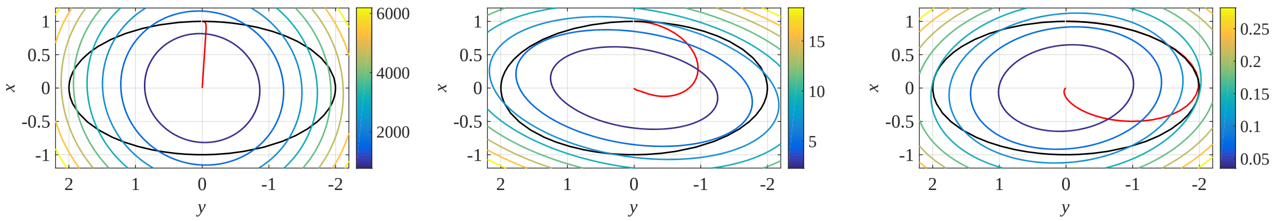

(a) $q = 3$. (b) $q = 0$. (c) $q = -3$.

Fig. 3. $t_f = 6$.

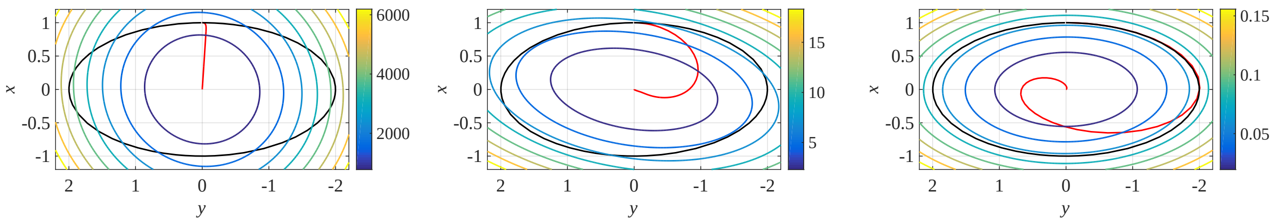

(a) $q = 3$. (b) $q = 0$. (c) $q = -3$.

Fig. 4. $t_f = 9$.

direction for $Q \to 0$. This is because the chaser can approach the origin by using the drift motion along y-axis. In Fig. 8, the optimal trajectory seems to exploit the drift motion along y-axis for small $q = -3$.

From the attractive set for the two situations, it can be said that the attractive set for small q reflect the dynamical structure of the motion since the optimal control exploits the natural motion of the system to reduce the control effort.

4.3. Discussion of a shape of an attractive set

For the LQR problem, the weight matrices for the performance index determine the relative importance between state and control input. From Figs. 2 - 4 and 6, it can be seen that the optimal trajectory and the shapes of the attractive sets depend on the weight matrices. As q varies, the shape and direction of the attractive set change and the optimal initial positions also move. Then the change in the shapes converges for sufficiently small q in Figs. 2(c), 3(c), 4(c), which concern more about control effort.

In Figs. 2(a), 3(a), 4(a), the weight on state is relative large ($q = 3$) and the shape of attractive set is circle. When the weight on state is relatively large, the optimal trajectory tends to take a shorter path to the origin. Actually, the distance to the origin is the shortest on the x-axis on the periodic solution of Hill 's equation. On the other hand, in Fig. 2(c), the attractive set for the case with $q = -3$ is ellipse which takes the optimal initial position on the y-axis. In this result, the time constraint is strong and the drift motion along y-axis might be used in this solution.

From Figs. 2(c), 3(c) and 4(c), it can be observed that the attractive sets converges to different shape for each t_f even for the same Q and R. Therefore, the final-time t_f is also an important factor to determine the optimal trajectory for the finite-time problem. Moreover, from the shapes of the attractive set, the optimal initial positions are uniquely determined from the attractive set for finite-time case. Therefore it can be said that the optimal solution is highly sensitive to the initial position for the short final-time problem. In other words, the coast arc solution is obtained for fixed final-time problem to reduce the control effort while coasting arc is not important for infinite-time problem.

4.3.1. Disccusion

Comparing Figs. 2(c), 3(c), 4(c), and Fig. 6(c), it is found that, when t_f is small, the shapes of the attractive sets for the fixed final-state, fixed final-time problem are different from that for the infinite-time problem. When the termination time is free

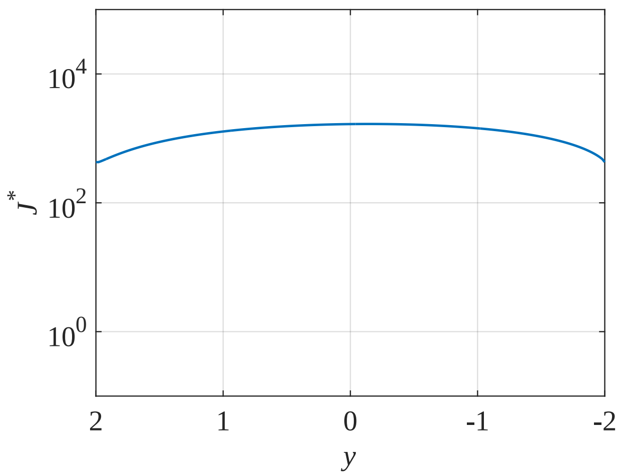

Fig. 5. Values of J^* on initial orbit when $q = -3$ and $t_f = 3$.

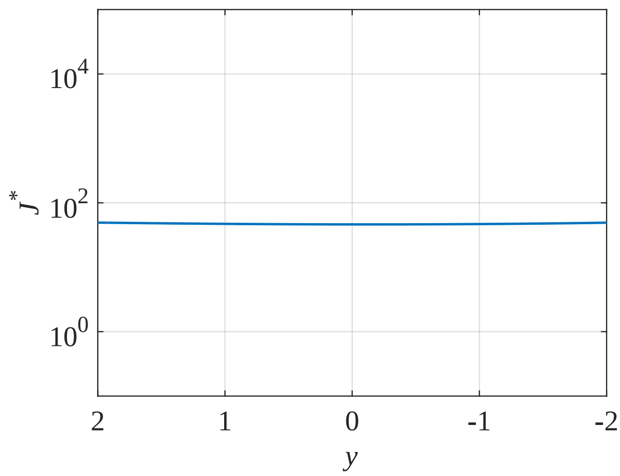

Fig. 7. Values of J^* on initial orbit when $q = -3$ and $t_f = \infty$.

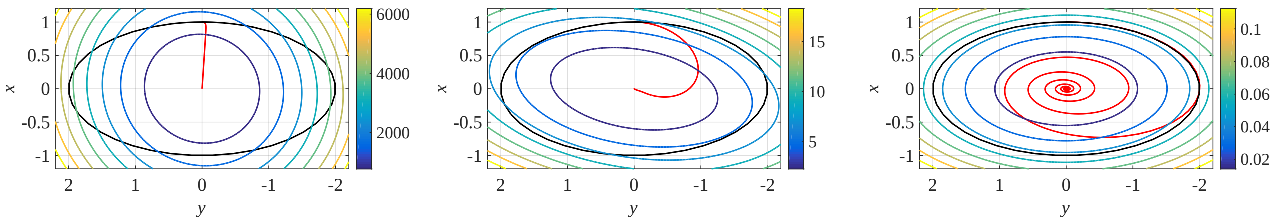

(a) $q = 3$. (b) $q = 0$. (c) $q = -3$.

Fig. 6. $t_f = \infty$.

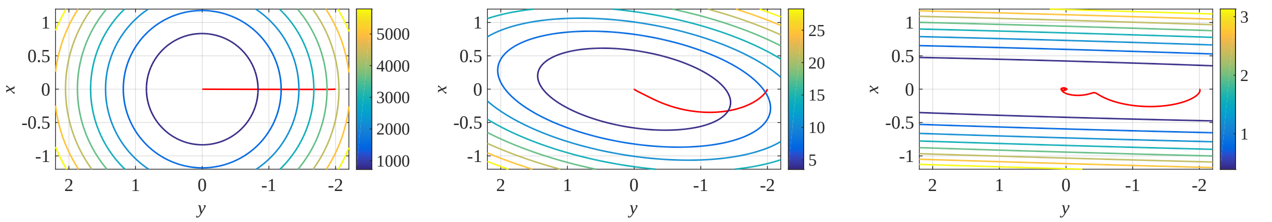

(a) $q = 3$. (b) $q = 0$. (c) $q = -3$.

Fig. 8. The contour of the attractive set for $x_0 = [x, y, 0, 0]$.

and the final state is $\boldsymbol{x}_f = \boldsymbol{0}$, the condition of t_f that minimizes J is as follows:[7)]

$$B^{\mathrm{T}} W^{-1}(t_0) U^{\mathrm{T}}(t_0) \boldsymbol{x}_0 = \boldsymbol{0} \quad (38)$$

$U^{\mathrm{T}}(t_0)$ and $W^{-1}(t_0)$ depend on t_f, so Eq. (38) is nothing but the condition of t_f.

Then $\boldsymbol{u}^*$ and J^* for the fixed final-state, fixed final-time problem are

$$\boldsymbol{u}^* = -R^{-1} B^{\mathrm{T}} S(t) \boldsymbol{x} \quad (39)$$

$$J^* = \boldsymbol{x}^{\mathrm{T}}(t_0) S(t_0) \boldsymbol{x}(t_0) \quad (40)$$

Comparing Eqs. (39) and (40), with Eqs. (26) and (29), it is found that the fixed final-state problem coincides the free final-state problem. Table 1 shows the magnitude of the vector given by the left-hand side of Eq. (38) in Figs. 2 to 4. For large t_f, the left-hand side of Eq. (38) becomes smaller. When the value of the left-hand side of Eq. (38) is large, the second term of Eq. (23)

$$-\boldsymbol{x}_0^{\mathrm{T}} U(t_0) W^{-1}(t_0) U^{\mathrm{T}}(t_0) \boldsymbol{x}_0$$

becomes large, which affects the shape of the attractive set.

Table 1. Values of L.H.S of Eq. (38)

	$Q = 10^3 \boldsymbol{I}$	$Q = \boldsymbol{I}$	$Q = 10^{-3} \boldsymbol{I}$	$Q = \boldsymbol{O}$
$t_f = 3$	3.3711	0.8097	1.3673	1.3684
$t_f = 6$	0.1674	0.0848	0.1695	0.1734
$t_f = 9$	0.0083	0.0088	0.0673	0.0852

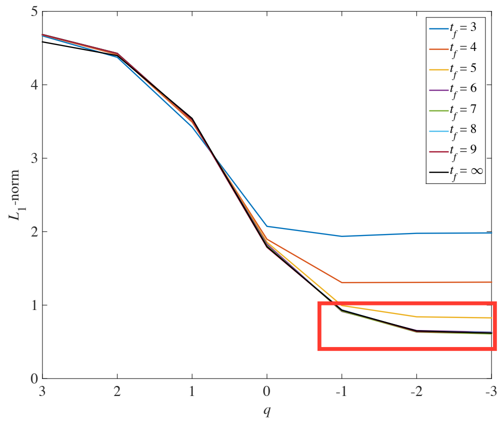

Fig. 9. L_1-norm vs. q.

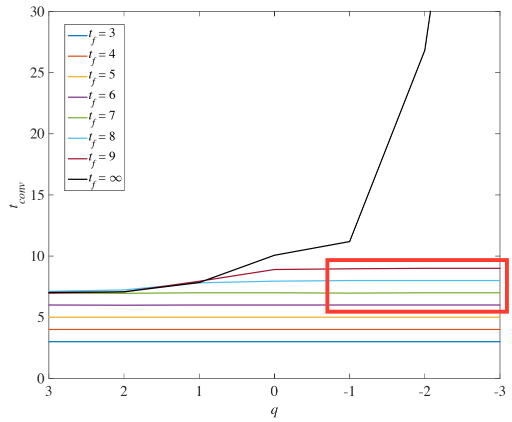

Fig. 10. t_{conv} vs. q.

4.4. Comparison of L_1-norm and rendezvous completion time

We evaluate the trajectory using the L_1-norm, which is proportional to the fuel consumption. The L_1-norm is defined as follows:

$$L_1 = \int_{t_0}^{t_f} |\boldsymbol{u}(t)| dt \tag{41}$$

We compare the L_1-norm with t_{conv} by changing the weight of the state. Figures 9 and 10 show the L_1-norm versus q and t_{conv} versus q, respectively.

First, as a general property, it is found that the L_1-norm decreases and t_{conv} increases with decreasing weight of the state. As shown in Fig. 9, the longer t_f is taken, L_1-norm becomes closer to the infinite-time problem. Additionally, as shown in Fig. 10, the rendezvous is completed in a finite time from around $q = 0$ in the fixed final-state, fixed final-time problem; in contrast, in the infinite-time problem, it does not become a constant value, but rather monotonically increases. For example, in Table 2 we show a summary of the L_1-norm and t_{conv} for $t_f = 9$ and $t_f = \infty$ when $q = -3$. Although the L_1-norms are almost equal, t_{conv} is much smaller in the fixed final-state, fixed final-time problem. It is assumed that, if the weight of the control input is sufficiently large for t_f, the fixed final-state, fixed final-time problem is superior in terms of equivalent L_1-norm and lower t_{conv}. Similarly, paying attention to the red square region in Figs. 9 and 10, it is found that the fixed final-state, fixed final-time problem is better than the infinite-time problem as t_{conv} is small even though L_1-norm is equal.

Table 2. Comparison of L_1-norm and t_f when $q = -3$.

	$t_f = 9$	$t_f = \infty$
L_1-norm	0.63	0.62
t_{conv}	9.0	69

5. Conclusion

This paper presents the properties of an attractive set for optimal control for different boundary conditions using a linear quadratic regulator. The analysis using the attractive set revealed the optimal initial state for the rendezvous problem under different formulation of optimal control problem. One of the interesting property of the attractive set for the infinite-time problem is that it reflect the natural solutions of the Hill's equations. It was found that the L_1-norm of the fixed final-state, fixed final-time problem is close to that of the infinite-time problem when the termination time is large. Therefore, the formulation using the fixed-final-state, fixed-final-time problem leads shorter rendezvous completion time with almost the same L_1-norm.

References

1) Kinoshita, H.: Celestial Mechanisms and Orbital Dynamics, Univ. of Tokyo Press, (1998) (in Japanese).
2) Kyle Alfriend, Srinivas Rao Vadali, Pini Gurfil, Jonathan How, Louis Breger, Spacecraft Formation Flying: Dynamics, control and Navigation, Butterworth-Heinemann (2009).
3) Kristiansen, Raymond and Nicklasson, Per Johan, Spacecraft formation flying: a review and new results on state feedback control, Acta Astronautica, Vol. 65, No. 11, pp. 1537-1552, (2009).
4) Motoyuki Shibata and Akira Ichikawa, Orbital Rendezvous and Flyaround Based on Null Controllability with Vanishing Energy, Journal of Guidance, Control, and Dynamics, Vol. 30, No. 4, pp. 934-945 (2007).
5) V. M. Guibout and D. J. Scheeres, Solving Relative Two-Point Boundary Value Problems: Spacecraft Formulation Flight Transfers Application, Journal of Guidance, Control, and Dynamics, Vol. 27, No. 4, 2004, pp. 693 - 704.
6) C. Park, V. M. Guibout, and D. J. Scheeres, Solving Optimal Continuous Thrust Rendezvous Problems with Generating Functions," Journal of Guidance, Control, and Dynamics, Vol. 29, No. 2, 2006, pp. 321 - 331.
7) Ohtsuka, T.: Introduction to Nonlinear Optimal Control, CORONA PUBLISHING CO., LTD. (2011) (in Japanese).
8) Anderson, Brian D.O. and Moore, J. B., Optimal Control: Linear Quadratic Methods, Courier Corporation, 2007
9) Tsuneo, Y. and Imura, J.: Modern Control Theory, Shokoudou Press, (1994) (in Japanese).
10) Bando, M. and Scheeres, D.J., Attractive Sets to Unstable Orbits Using Optimal Feedback Control, Journal of Guidance, Control, and Dynamics, Vol. 39, No. 12, pp. 2725-2739, 2016